Magnetic Detonation in Crystals of Nanomagnetics

O. Yukhimenko[1], M. Modestov[2,3], V. Bychkov[1], and M. Mattias[1,4]

[1]Department of Physics, Umeå University, Umeå, Sweden
[2]Nordita, KTH Royal Institute of Technology and Stockholm University, Stockholm, Sweden
[3]Department of Mechanical and Aerospace Engineering, Princeton University, Princeton, USA
[4]Department of Applied Physics, Chalmers University of Technology, Göteborg, Sweden

1 Inroduction

Presently, there is much interest in molecular (nano)magnets with unique superparamagnetic properties, which may be used for quantum computing and memory storage [1-4]. A remarkable feature of nanomagnets is that these macromolecules with large effective molecular spin (e.g., $S = 10$ for Mn_{12}-acetate) can keep their spin orientation upon the reversal of the external magnetic field [3,4]. Because of the strong molecular anisotropy, the spin of a nanomagnet is directed preferentially along the so-called easy axis of the crystal, and it leads to a considerable energy barrier between the spin-up and spin-down states. At low temperatures, in a magnetic field directed along the easy axis, the states with spin along the field and against the field become stable and metastable, respectively. The energy difference between the two states is determined by the Zeeman energy Q, as illustrated in Fig. 1, with the energy barrier designated by E_a. The barrier hinders spontaneous transition from the metastable to stable state at low temperatures [4,5], so that fast spin flipping requires help from outside.

For nanomagnets composing a crystal, relatively fast spin flipping of one particular molecule may beinduced by energy supplied by its neighbors. When all or most of the molecules of a crystal are initially in the metastable state, then local heating by an external source may trigger local spin flipping, with Zeeman energy released in the heated region and transported to the next layer of the crystal [2,6-10]. The released heat facilitates spin flipping in the next layer, so that the process spreads in a crystal as a thin, self-supporting magnetization front. In such a front thermal energy is transported by means of thermal conduction and the total front propagates at moderate speed, 1-10 m/s [2,6]. Due to the striking similarity of such avalanches to slow combustion flame, this phenomenon has been called magnetic deflagration.

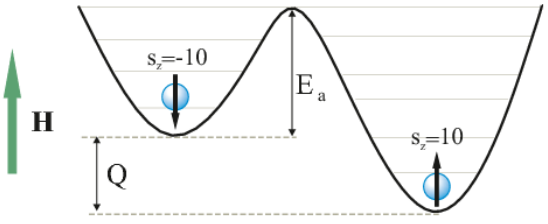

Figure 1: Schematic representation of the double-well structure of a nanomagnet in an external magnetic field.

Correspondence to: modestov@princeton.edu

In contrast to the slow magnetic deflagration studied in the absolute majority of works on the subject [2,6-8], recent experiments presented in Ref. [9] detected ultrafast spin avalanches propagating at a speed comparable to the sound speed in the crystals, ≈ 2000 m/s. The theory presented in Ref. [10] has explained the ultrafast spin avalanches in terms of "magnetic detonation" and has investigated the key properties of the process. In particular, it has been demonstrated that magnetic detonation belongs to the type of weak detonations and propagates with speed only slightly exceeding the sound speed. Reference [10] has also studied the structure of magnetic detonation within the traditional combustion model of a detonation front consisting of an infinitely thin leading shock and a zone of energy release of finite thickness [11].

The purpose of the present work is to provide an accurate description of the magnetic detonation structure in crystals of nanomagnets by taking into account thermal conduction and volume viscosity. We point out that, unlike commonly known shear viscosity arising due to the relative motion of gas or fluid layers, volume viscosity describes momentum and energy dissipations due to compression of a medium. While shear viscosity is not typical for solid-state processes such as magnetic detonation in the crystals of nanomagnets, volume viscosity has to be considered. Here we show that the transport processes result in smooth profiles of the most important thermodynamic crystal parameters, such as temperature, density, and pressure, all over the magnetic detonation front, including the leading shock.

2 Basic features of magnetic detonation

Here we are interested in a planar stationary one-dimensional detonation wave propagating with constant supersonic speed D. Although we deal with the solid state physics, propagation of shocks and detonations in crystals of nanomagnets are also described by hydrodynamic conservation laws of mass, momentum, and energy similar to gaseous detonation [11].

$$\rho_0 D = \rho u, \tag{1}$$

$$P_0 + \rho_0 D^2 = P + \rho u^2, \tag{2}$$

$$\varepsilon_0 + \frac{P_0}{\rho_0} + \frac{1}{2}D^2 + Q = \varepsilon + \frac{P}{\rho} + \frac{1}{2}u^2 + Qa, \tag{3}$$

where ε is the thermal energy per unit mass, Q stands for the Zeeman energy release, and a is the fraction of molecules in the metastable state; the label 0 designates the initial state. The conservation laws Eqs. (1)–(3) have to be complemented by an equation of state. It is convenient to define a new dimensionless value $r \equiv \rho/\rho_0 = V_0/V$, which describes the crystal compression in the process. Weak shock and detonation cause only elastic deformations so that the crystal state equation can be written as a combination of elastic and thermal components as [7,12]

$$\frac{P}{\rho_0} = \frac{c_0^2}{n}\left(r^n - 1\right) + \frac{1}{\alpha+1}\frac{R}{M}\frac{A\Gamma k_B}{\Theta_D^\alpha}T^{\alpha+1}r, \tag{4}$$

$$\varepsilon = \frac{c_0^2}{n}\left(\frac{r^n - 1}{n-1} + \frac{1}{r} - 1\right) + \frac{1}{\alpha+1}\frac{R}{M}\frac{A}{\Theta_D^\alpha}T^{\alpha+1}, \tag{5}$$

where $c_0 \approx 2000$ m/s is the sound speed in the crystal, the power exponent $n \approx 4$ as suggested in [12], $\Gamma \approx 2$ is the Gruneisen coefficient, $\alpha = 3$ stands for dimension of the problem, $\Theta_D = 38$ K is the Debye temperature for $\mathrm{Mn_{12}}$, k_B is the Boltzmann constant, coefficient $A = 12\pi^4/5$ corresponds to the simple crystal lattice. In the above equations the thermal conduction and viscous forces have been omitted, their influence will be described in the next section. The Zeeman energy Q and the activation energy E_a

are determined by the applied magnetic field and can be obtained from the system Hamiltonian [6] as

$$Q = 2g\mu_B \frac{R}{M} S_z B_z, \tag{6}$$

$$E_a = D_a S_z^2 - g\mu_B S_z B_z + \frac{g^2 m u_B^2}{4D_a} H_z^2, \tag{7}$$

where $g \approx 2$ is the gyromagnetic factor, μ_B is the Bohr magneton, R is the ideal-gas constant, $M = 1868$ g/mol is the molecular mass, S_z is the spin projection ($S_z = -10$ for metastable and $S_z = 10$ for stable states), B_z is the magnetic field directed along the easy axis of the crystal, and $D = 0.65$ K is the magnetic anisotropy constant. According to those expressions the Zeeman energy increases linearly with the magnetic field, while the activation energy decreases and becomes zero at $B_z \approx 10$ T, at higher fields the potential barrier, shown in Fig. 1 disappears and all the molecules settle on the stable level with $S_z = 10$.

The properties of shocks (detonations) are usually represented by the Hugoniot (detonation) curves $P = P(V)$, which show all possible final states behind a shock, determined by Eqs. (1-5) for a given initial state and energy release. We reduce Eqs. (1-5) to a single equation for pressure as

$$\left(\frac{1}{\Gamma} - \frac{r-1}{2}\right)\frac{P}{\rho_0} = rQ(1-a) + \left(r + \frac{r-1}{2}\Gamma\right)\varepsilon_0 + \frac{c_0^2}{n-1}\left[r - 1 - \left(1 - \frac{n-1}{\Gamma}\right)\frac{r^n - 1}{n}\right]. \tag{8}$$

In the case of zero energy release, $a = 1$, Eq. (8) describes the Hugoniot curve for a shock wave (label *s*). The leading shock compresses the crystal with corresponding increase in density, pressure, and temperature. The temperature increase initiates spin flipping (similar to chemical reaction in combustion) with the Zeeman energy release. The released energy provides expansion of the medium, acting as a piston, supporting the leading shock. In the case of complete spin reversal, $a = 0$, Eq. (8) describes the final state behind the detonation front (label *d*). The Hugoniot and detonation curves obtained using Eq. (8) are shown in Fig. 2 for $B_z = 4$ T. Due to the energy release, the detonation curve is always above the Hugoniot one. In the case of Mn_{12} we find that the elastic contribution to the pressure and energy dominates over the thermal one, which leads to a rather weak detonation with the shock and detonation curves almost coinciding, see the inset of Fig. 2.

A self-supporting detonation corresponds to the Chapman-Jouguet (CJ) regime, for which velocity of the products in the reference frame of the front is equal to the local sound speed [11]. The CJ point at the detonation curve is determined by the tangent line connecting the initial state and the detonation curve. Since the detonation and Hugoniot curves are extremely close, the intersection of the tangent line cannot be seen in the traditional representation of the curves. In order to make the figure illustrative, we subtract this tangent line from the Hugoniot and detonation curves in Fig. 2. In the new representation, the tangent line corresponds to the zero line, while the Hugoniot and detonation curves may be distinguished quite well. Changes of the crystal parameters in the CJ detonation are indicated by the bold line with arrows: the parabolic piece of

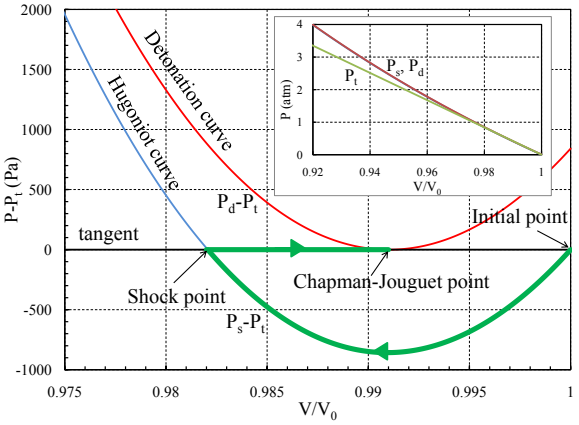

Figure 2: The insert: Traditional presentation of the Hugoniot and detonation curves and the tangent line to the detonation curve in Mn_{12}-acetate for the external magnetic field $H_z = 4$ Tesla. The main plot: The Hugoniot and detonation curves with the tangent line extracted; label "t" stands for tangent.

the line shows modifications within the leading shock, while the straight piece describes the Zeeman energy release in the detonation behind the shock until the spin reversal is complete in the final CJ point.

From Fig. 2 we see that the magnetic detonation compresses the Mn_{12}crystal very slightly ($< 2\%$), which allows us to derive an analytical expressions for detonation parameters using expansion $r = 1 + \delta$ with $\delta << 1$. In such a way we find that the final compression can be computed as

$$\delta_d = \frac{1}{c_0}\sqrt{\frac{2\Gamma Q}{n+1}}, \tag{9}$$

while the compression behind the leading shock is twice larger, $\delta_s \approx 2\delta_d$. The detonation speed may be found from Eq. (1) and Eq. (9), as

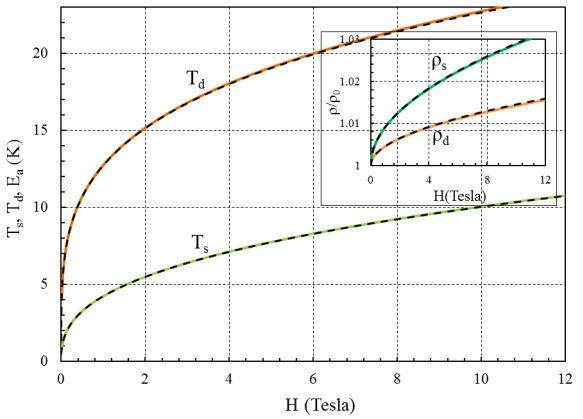

Figure 3: Temperature and density at the leading shock and behind the detonation front versus the external magnetic field. Solid lines show exact numerical solution; the dashed lines stand for the analytical theory Eq. (9) and Eq. (11).

$$D \approx c_0 + \sqrt{\frac{n+1}{2}\Gamma Q}. \tag{10}$$

The second term in the right-hand side of Eq. (11) is less than 2% with magnetic field under 4 T, being an example of very weak detonation wave as compared with regular combustion. Finally the temperature at the detonation wave may be determined as

$$T_d^{\alpha+1} = (\alpha+1)\frac{MQ\Theta_D^{\alpha}}{RA}\left(1 + \frac{7\Gamma}{12c_0}\sqrt{\frac{2\Gamma Q}{n+1}}\right). \tag{11}$$

We plot temperature and density at the shock and behind the detonation front in Figure 3. Together with approximate expressions from Eqs. (9-10) we also present exact solution to the whole set of equations (1-5), which almost coincide with the analytical solutions.

3 Detonation front structure with heat conduction and volume viscosity

In order to take into account volume viscosity and heat conduction, we rewrite the equations of momentum, and energy conservation for magnetic detonation as

$$P_0 + \rho_0 D^2 = P + \rho u^2 - \eta\frac{du}{dx}, \tag{12}$$

$$\rho_0 D\left(\varepsilon_0 + \frac{P_0}{\rho_0} + \frac{1}{2}D^2 + Q\right) = \rho u\left(\varepsilon + \frac{P}{\rho} + \frac{1}{2}u^2\right) - \kappa\frac{dT}{dx} - \eta u\frac{du}{dx}. \tag{13}$$

The equation for mass conservation does not change. The internal structure of magnetic detonation can be obtained by integrating the equation for kinetics of spin relaxation [6], which strongly resembles the Arrhenius law of chemical kinetics. In the reference frame of the stationary magnetic detonation front, it can be written as

$$u\frac{\partial a}{\partial x} = -\frac{a}{\tau}exp\left(-\frac{E_a}{T}\right), \tag{14}$$

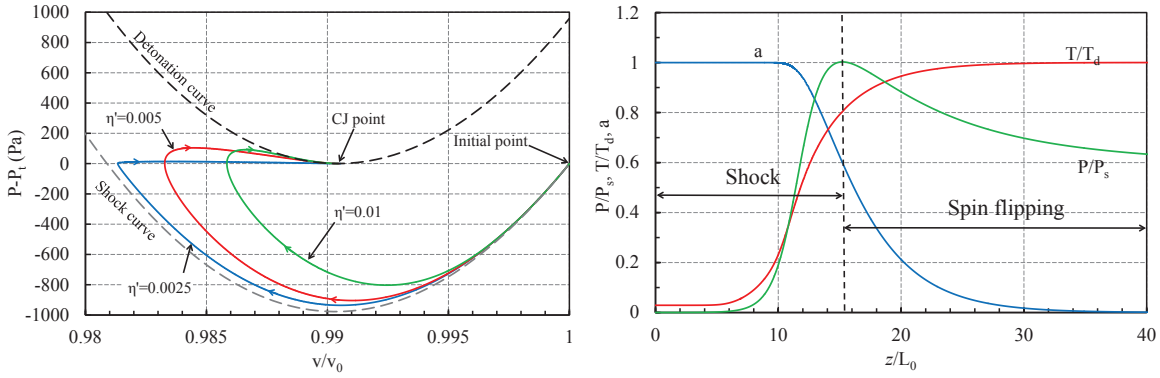

Figure 4: (Left) Pressure-volume diagram for different values of the scaled viscosity $\eta\prime = 0.0025,\ 0.005,\ 0.01$ in external magnetic field $B_z = 4$ T. (Right) Profiles of scaled pressure, temperature, and fraction of nanomagnets in the metastable state for magnetic detonation for scaled viscosity $\eta\prime = 0.05$ in the external magnetic field $B_z = 4$ T.

where $\tau \sim 10^{-7}$ s is a constant of time dimension characterizing the spin reversal [2,7]. We have found that thermal conduction influences slightly the temperature profile in magnetic detonation, with a very minor effect on density and pressure and with negligible modifications of the total front thickness. Much more dramatic modifications of the magnetic detonation structure are expected because of volume viscosity.

It is convenient to characterize the role of viscosity by the dimensionless parameter

$$\eta\prime \equiv \frac{\eta}{\rho_0 c_0 L_0} = \frac{\eta}{\rho_0 c_0^2 \tau}, \tag{15}$$

which plays a role similar to the inverse Reynolds number in fluid mechanics [11]. To the best of our knowledge, there have been no works, either experimental or theoretical, investigating volume viscosity in crystals of nanomagnets, and therefore we will take $\eta\prime$ as a free parameter. In particular, the parameter values $\eta\prime = 0.0025,\ 0.005,\ 0.01$ employed below correspond to the domain of Reynolds numbers $Re = 10200$, at such values of the Reynolds number gas and fluid flows are typically laminar.

In case of small finite values of volume viscosity $\eta\prime \sim 0.01$ the pressure-volume diagram, presented in Fig. 2 changes significantly, as demonstrated in Fig. 4a. We observe that all discontinuous jumps of the previous model [10] are replaced by continuous transition lines from the initial point to the CJ detonation products. For very small viscosity, $\eta\prime = 0.005$, the transition line (blue), although continuous, goes pretty close to the Hugoniot curve for the shock and then to the tangent line for the spin-flipping process. As we take larger values of volume viscosity, deviation of the pressure-volume plots from the discontinuous shock model becomes much more pronounced. The internal detonation front structure also exhibits continuous transition of all flow quantities from initial to final state, as shown in Fig. 4b.

It leads to another interesting aspect that is the very definition of a shock as a part of the magnetic detonation front becomes ambiguous when volume viscosity is taken into account. To avoid the ambiguity, we notice that within the model of a discontinuous shock, the pressure maximum is attained at the shock front, and then pressure goes down as the spin flipping starts. In the same way it seems natural to treat the point of maximal pressure in Figs. 4b and 5 as the back side of the shock region. In Fig. 5 we present pressure profiles for several values of the scaled viscosity, choosing $z = 0$ as the position of the pressure maximum and hence the back side of the shocks. Then the regions corresponding to $z < 0$ belong to the shocks smoothed by viscosity, while the domain of $z > 0$ may be treated roughly as the regions of spin flipping with Zeeman energy release.

It should also be mentioned that the experimentally employed sample sizes for the crystals of nanomagnets are about 2 mm (e.g., see Refs. [2,9]). As a result, it is rather difficult to observe steady, well-developed magnetic detonation in common experimental conditions since such observations require samples much larger than the detonation front thickness. Instead, we suggest that most of the experimental points reported in Ref. [9] for ultrafast magnetic avalanches correspond to magnetic detonation in the process of development, which is also indicated by the average avalanche speed in the samples being noticeably below the sound speed. Then, in order to observe a well-developed magnetic detonation one has to perform experiments with much bigger crystals of nanomagnets, simultaneously reducing the detonation front thickness as much as possible. In the case of relatively small viscosity, $\eta\prime = 0.005$, the detonation front thickness may be reduced by decreasing the scaled activation energy of spin flipping E_a/T_s. This, in turn, may be achieved by increasing the external magnetic field B_z or by adding a transverse-magnetic-field component B_x. In some respects the transverse field also mimics the presence of the transverse-magnetic anisotropy, which may lead to splitting of spin states even at zero magnetic field and, consequently, to changing the activation energy. Another important feature of the experimental observations of Ref. [11] is that the ultrafast avalanches were obtained for the magnetic field close to the quantum resonance values of the nanomagnets. Quantum resonances lead to a strong decrease in the factor τ in the kinetic equation of spin flipping, Eq. (14), and hence of the characteristic width of the magnetic detonation front, which may allow experimental observation of magnetic detonation.

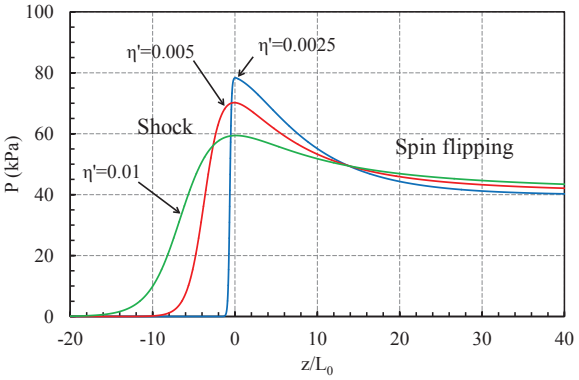

Figure 5: Pressure profiles in magnetic detonation for different values of the scaled viscosity, external magnetic field $B_z = 4$ T.

References

[1] J. Tejada, E. M. Chudnovsky, E. del Barco, J. M. Hernandez, and T. P. Spiller, Nanotechnology 12, 181 (2001).

[2] Y. Suzuki *et al.*, Phys. Rev. Lett. 95, 147201 (2005).

[3] R. Sessoli, D. Gatteschi, A. Caneschi, and M. A. Novak, Nature (London) 365, 141 (1993).

[4] J. R. Friedman, M. P. Sarachik, J. Tejada, and R. Ziolo, Phys. Rev. Lett. 76, 3830 (1996).

[5] E. M. Chudnovsky and J. Tejada, Macroscopic Quantum Tunneling of the Magnetic Moment (Cambridge University Press, Cambridge, 1998).

[6] D. A. Garanin and E. M. Chudnovsky, Phys. Rev. B 76, 054410 (2007).

[7] M. Modestov, V. Bychkov, and M. Marklund, Phys. Rev. B 83, 214417 (2011).

[8] O. Jukimenko, C. M. Dion, M. Marklund, and V. Bychkov, Phys. Rev. Lett. 113, 217206 (2014).

[9] W. Decelle *et al.*, Phys. Rev. Lett. 102, 027203 (2009).

[10] M. Modestov, V. Bychkov, and M. Marklund, Phys. Rev. Lett. 107, 207208 (2011).

[11] C. K. Law, Combustion Physics (Cambridge University Press, Cambridge, 2006).

[12] Ya. B. Zeldovich and Yu. P. Raizer, Physics of Shock Waves and High-Temperature Hydrodynamic Phenomena (Dover, Mineola, NY, 2002).